PNAS INAUGURAL ARTICLE | IMMUNOLOGY AND INFLAMMATION

Caspase-8 and FADD prevent spontaneous ZBP1 expression and necroptosis

Diego A. Rodriguez[a], Giovanni Quarato[a], Swantje Liedmann[a], Bart Tummers[a], Ting Zhang[b], Cliff Guy[a], Jeremy Chase Crawford[a], Gustavo Palacios[a], Stephane Pelletier[a], Halime Kalkavan[a], Jeremy J. P. Shaw[a], Patrick Fitzgerald[a], Mark J. Chen[a], Siddharth Balachandran[b], and Douglas R. Green[a,1]

This article is part of the special series of Inaugural Articles by members of the National Academy of Sciences elected in 2022.
Edited by Julie Blander, Weill Cornell Medicine, New York, NY; received April 26, 2022; accepted August 23, 2022 by Editorial Board Member Carl F. Nathan

The absence of Caspase-8 or its adapter, Fas-associated death domain (FADD), results in activation of receptor interacting protein kinase-3 (RIPK3)- and mixed-lineage kinase-like (MLKL)–dependent necroptosis in vivo. Here, we show that spontaneous activation of RIPK3, phosphorylation of MLKL, and necroptosis in Caspase-8– or FADD-deficient cells was dependent on the nucleic acid sensor, Z-DNA binding protein-1 (ZBP1). We genetically engineered a mouse model by a single insertion of FLAG tag onto the N terminus of endogenous MLKL ($Mlkl^{FLAG/FLAG}$), creating an inactive form of MLKL that permits monitoring of phosphorylated MLKL without activating necroptotic cell death. $Casp8^{-/-}$ $Mlkl^{FLAG/FLAG}$ mice were viable and displayed phosphorylated MLKL in a variety of tissues, together with dramatically increased expression of ZBP1 compared to $Casp8^{+/+}$ mice. Studies in vitro revealed an increased expression of ZBP1 in cells lacking FADD or Caspase-8, which was suppressed by reconstitution of Caspase-8 or FADD. Ablation of ZBP1 in $Casp8^{-/-}$ $Mlkl^{FLAG/FLAG}$ mice suppressed spontaneous MLKL phosphorylation in vivo. ZBP1 expression and downstream activation of RIPK3 and MLKL in cells lacking Caspase-8 or FADD relied on a positive feedback mechanism requiring the nucleic acid sensors cyclic GMP-AMP synthase (cGAS), stimulator of interferon genes (STING), and TBK1 signaling pathways. Our study identifies a molecular mechanism whereby Caspase-8 and FADD suppress spontaneous necroptotic cell death.

necroptosis | ZBP1 | MLKL | caspase-8 | interferon

Significance

Caspase-8 and Fas-associated death domain (FADD) play key roles in the regulation of cell death by necroptosis. The absence of either protein results in early embryonic lethality due to the activation of the kinase receptor interacting protein kinase-3 (RIPK3) and its phosphorylation of the necroptosis executioner, mixed-lineage kinase-like (MLKL). We genetically engineered and characterized a mouse model to monitor MLKL phosphorylation in the absence of necroptosis in vivo. Ablation of caspase-8 or FADD resulted in the transcriptional upregulation in several tissues of Z-DNA binding protein-1 (ZBP1), a cytosolic nucleic acid sensor capable of activating RIPK3, and ZBP1 was required for spontaneous phosphorylation of MLKL. Our findings provide a mechanism by which the FADD/Caspase-8 complex prevents necroptosis.

Necroptosis is a regulated, necrotic cell death process that depends on the phosphorylation of the pseudokinase, mixed-lineage kinase-like (MLKL) by receptor interacting kinase-3 (RIPK3) (1, 2). RIPK3 is activated by three known mechanisms. Under conditions that permit necroptosis to proceed (see next paragraph), ligation of tumor necrosis factor receptor-1 (TNFR1) activates RIPK1, which in turn binds to RIPK3 via shared RIP homology interaction motifs (RHIM) present in both molecules (3, 4). Similarly, engagement of Toll-like receptors (TLR)-3 and -4 recruits the adapter, TIR domain-containing adapter-inducing interferon-β (TRIF), which has a RHIM that is capable of binding and activating RIPK3 (5). Finally, the cytosolic nucleic acid sensor, Z-DNA binding protein-1 (ZBP1) also contains a RIPK3-activating RHIM (6, 7). Despite its name, ZBP1 senses Z-RNA rather than Z-DNA (8–10) and mediates cell death upon infections with orthomyxoviruses (11, 12), herpesviruses (6), and poxviruses (8, 13).

Fas-associated death domain (FADD) is an adapter that is engaged by TNFR1 ligation as well as by active RIPK1, and this functions to bind and activate the caspase protease, Caspase-8 (14, 15). The FADD/Caspase-8 complex proteolytic activity inhibits necroptosis in each of the settings wherein RIPK3 can be activated. This inhibition is important during embryogenesis and in adult tissues, as evidenced by the ability of RIPK3 or MLKL ablation to protect mice from the catastrophic effects of deletion of FADD or Caspase-8 during embryogenesis (15, 16) or upon acute deletion in adult tissues (17). Cleavage of RIPK1 by Caspase-8 is essential for murine and human homeostasis (18), as mice or humans in which the cleavage site is inactivated die during embryogenesis (mice) or display lethal inflammatory disease after birth (humans) (19, 20).

FADD/Caspase-8–mediated proteolytic cleavage of RIPK1 prevents necroptosis induced by ligation of TNFR1 (15), as RIPK1 is required for the activation of RIPK3 in this setting. Unlike the induction of necroptosis by ligation of TNFR1, ZBP1 activates RIPK3 independently of RIPK1 (21). Therefore, how FADD/Caspase-8 prevents ZBP1-induced necroptosis remains unresolved. Here we describe studies in which cells or

Author contributions: D.A.R., G.Q., S.L., B.T., S.B., and D.R.G. designed research; D.A.R., G.Q., S.L., B.T., T.Z., C.G., J.C.C., G.P., H.K., and J.J.P.S. performed research; G.Q., T.Z., G.P., S.P., and P.F. contributed new reagents/analytic tools; D.A.R., S.L., B.T., J.C.C., M.J.C., and D.R.G. analyzed data; and D.A.R. and D.R.G. wrote the paper.

Competing interest statement: D.R.G. consults for Ventus Pharmaceuticals, Inzen Pharmaceuticals, and Horizon Pharmaceuticals.

J.B. is a guest editor invited by the Editorial Board.

[1]To whom correspondence may be addressed. Email: douglas.green@stjude.org.

This article contains supporting information online at http://www.pnas.org/lookup/suppl/doi:10.1073/pnas.2207240119/-/DCSupplemental.

Published October 3, 2022.

animals lacking functional MLKL and either FADD or Caspase-8 sustain active RIPK3 activity that depends, in large part, on the expression of ZBP1, which we found to be highly expressed in the double-deficient cells and animal tissues. In the presence of FADD and Caspase-8, this constitutive expression of ZBP1 is suppressed. We identify the nucleic acids sensors cyclic GMP-AMP synthase (cGAS) and stimulator of interferon genes (STING) as responsible for ZBP1 expression in cells lacking FADD or Caspase-8.

Results

FADD/Caspase-8 Inhibits Spontaneous RIPK3-MLKL Pathway Activity. Because ablation of MLKL in mice lacking either Caspase-8 or FADD allows these otherwise embryonically lethal genotypes to mature into adults (16), it is reasonable to assume that one or more signaling pathways that activate RIPK3 (and therefore MLKL and necroptotic death) are active during embryogenesis. Similarly, tissue damage to the gut or skin by acute ablation of *casp8* in adult animals is prevented by ablation of either RIPK3 or MLKL (16, 17, 22), further suggesting that the RIPK3 activation signals are present in these adult tissues (16, 23). To identify these signals, we generated mouse embryonic fibroblasts (MEF) from $Casp8^{-/-}Mlkl^{-/-}$ or $Fadd^{-/-}Mlkl^{-/-}$ embryos and examined the phosphorylation of RIPK3 (Fig. 1*A* and *SI Appendix*, Fig. S1*A*). In the absence of either FADD or Caspase-8, RIPK3 was constitutively phosphorylated. Ectopic reexpression of FADD or Caspase-8 suppressed phospho-RIPK3 (Fig. 1*A* and *SI Appendix*, Fig. S1*A*). Phosphorylation of RIPK1 showed a similar pattern (Fig. 1*A*). We then engineered these immortalized MEF to inducibly express MLKL with a C-terminal FLAG (iMLKL-FLAG) in response to doxycycline (Dox) (23). Treatment with Dox rapidly induced cell death that was suppressed by enforced expression of FADD or

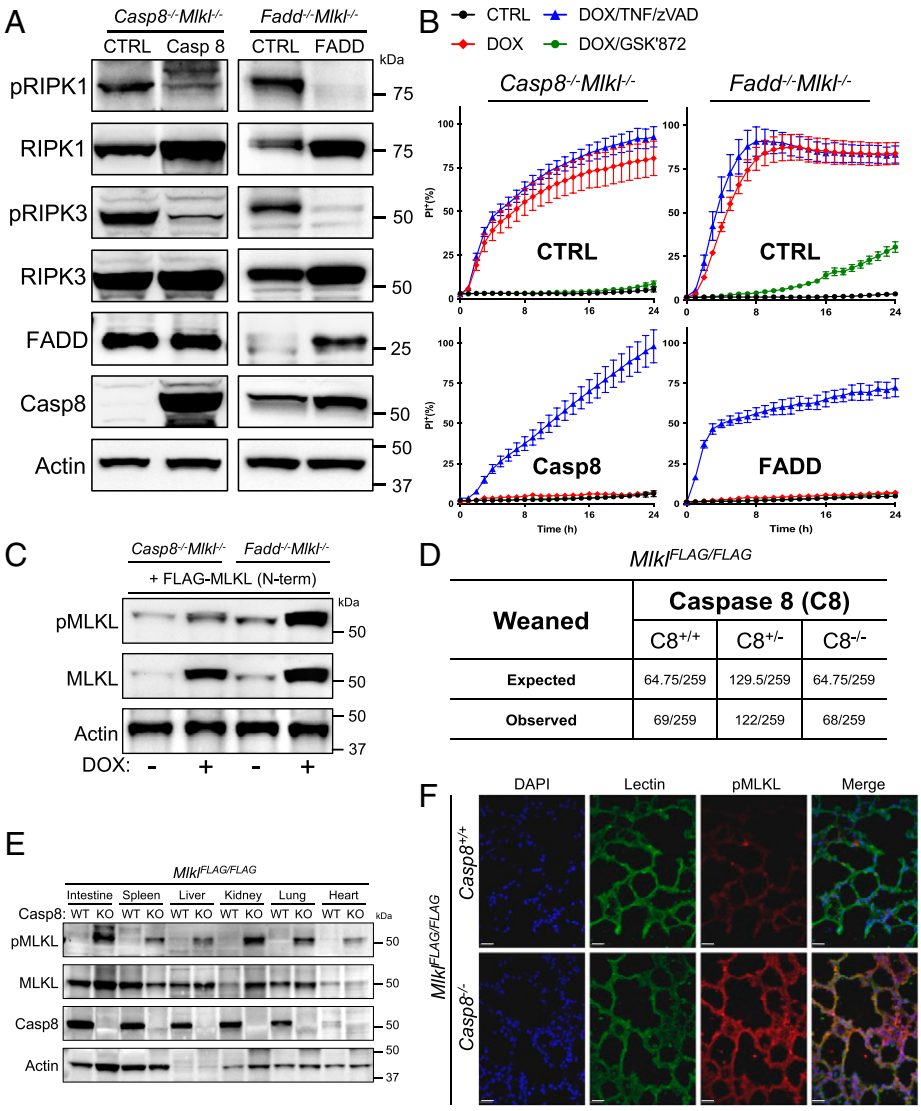

Fig. 1. *Fadd* or *Casp8* absence promotes constitutive RIPK3-MLKL pathway activity. (*A*) $Fadd^{-/-}Mlkl^{-/-}$ or $Casp8^{-/-}Mlkl^{-/-}$ MEF were reconstituted with empty vector (CTRL), FADD, or Caspase-8 (Casp8), respectively. Cell lysates were collected and phosphorylation of RIPK1, RIPK3, and all reconstituted components were assessed by immunoblotting. (*B*) Cells as shown in *A* were reconstituted with Dox-inducible MLKL-FLAG (C terminal; iMLKL-FLAG) and incubated with Dox (1 μg/mL) in the absence or presence of GSK'872 (1 μM) or TNF (10 ng/mL) plus zVAD (50 μM). Kinetics of cell death was monitored by propidium iodide (PI^+ %) uptake using an Incucyte Kinetic Live Cell Imager. (*C*) Cells as shown in *A* were reconstituted with Dox-inducible FLAG-MLKL (N terminal). Cell lysates were analyzed by immunoblotting using indicated antibodies. (*D*) Expected Mendelian ratios and observed numbers of offspring from $Mlkl^{FLAG/FLAG}Casp8^{+/-}$ intercrosses. All observed genotypes reached adulthood. (*E*) Tissues from 4- to 6-wk-old $Mlkl^{FLAG/FLAG}Casp8^{+/+}$ or $Mlkl^{FLAG/FLAG}Casp8^{-/-}$ mice were examined by immunoblotting using indicated antibodies. (*F*) Immunofluorescence analysis of phospho-MLKL (pMLKL) from cryopreserved lung sections from animals as shown in *E*. (Scale bars, 10 μm.)

Caspase-8 in the corresponding cell line (Fig. 1*B*). The latter cells, which did not die in response to MLKL expression, nevertheless died upon treatment with Dox plus the caspase inhibitor carbobenzoxy-valyl-alanyl-aspartyl-[O-methyl]-fluoromethylketone (zVAD) and either TNF (Fig. 1*B* and *SI Appendix*, Fig. S1*D*) or poly I:C (*SI Appendix*, Fig. S1*E*), as expected (23).

To examine the phosphorylation of MLKL in these settings, we took advantage of the ability of an N-terminal FLAG to block the necroptotic function of MLKL without affecting its phosphorylation by RIPK3 (Fig. 1*C* and *SI Appendix*, Fig. S1*A*) (24). The phosphorylation of MLKL, as well as cell death induced in $Fadd^{-/-}Mlkl^{-/-}$ MEF upon reexpression of MLKL, was blocked by the RIPK3 inhibitor, GSK′872 (Fig. 1*B* and *SI Appendix*, Fig. S1 *B* and *C*), but not by the RIPK1 inhibitor, Necrostatin-1s (Nec-1s) (*SI Appendix*, Fig. S1 *B* and *C*). $Fadd^{-/-}Mlkl^{-/-}$ or $Casp8^{-/-}Mlkl^{-/-}$ cells reconstituted with a Dox-inducible FLAG-MLKL (iFLAG-MLKL) were treated with Dox and the expressed MLKL was assessed with an antibody to Phospho-S^{345} (24) by immunoblot (Fig. 1*C* and *SI Appendix*, Fig. S1*B*) and immunofluorescence (*SI Appendix*, Fig. S1*F*). The phosphorylation of MLKL in these settings was blocked by the RIPK3 inhibitor GSK′872 and was not enhanced by further addition of either TNF or poly I:C (*SI Appendix*, Fig. S1*G*). Thus, MEF lacking either FADD or Caspase-8 display constitutive RIPK3 activity capable of phosphorylating MLKL and driving necroptosis.

We generated a mouse in which a FLAG tag was appended onto the N terminus of endogenous MLKL (*SI Appendix*, Fig. S1*H*). To formally test the idea that FLAG-MLKL is inactive, but can still be phosphorylated and form a complex with RIPK3 (23, 24), we crossed these animals with mice harboring a null allele of *casp8*. The intercross of $Casp8^{+/-}Mlkl^{FLAG/FLAG}$ mice resulted in homozygous $Casp8^{-/-}Mlkl^{FLAG/FLAG}$ mice that weaned at the expected Mendelian frequency (Fig. 1*D*). Thus, FLAG-MLKL acts as a null allele to prevent embryonic death of $casp8^{-/-}$ mice (16). This mouse model allowed us to examine the phosphorylation status of MLKL in $Casp8^{-/-}Mlkl^{FLAG/FLAG}$ tissues ex vivo. Strikingly, every tissue we examined accumulated high levels of phospho-MLKL (Fig. 1*E*), although we cannot conclude that this was the case for all cell types in those tissues. However, immunohistochemistry of the lung (Fig. 1*F*) revealed robust phospho-MLKL staining in alveolar cells that was absent in the lungs of $Casp8^{+/+}Mlkl^{FLAG/FLAG}$ mice.

The Absence of Caspase-8 or FADD Promotes Expression of ZBP1. In an effort to identify the source of the RIPK3-activating signal, we performed RNA-sequencing (RNA-seq) using $Fadd^{-/-}Mlkl^{-/-}$ or $Casp8^{-/-}Mlkl^{-/-}$ MEF with or without ectopically expressed FADD or Caspase-8, respectively. Among the mRNAs suppressed by FADD and Caspase-8, we noted the presence of *Zbp1* (Fig. 2*A*), whose product, ZBP1, is known to bind and activate RIPK3 (25). We confirmed that expression of both *Zbp1* mRNA (Fig. 2*B*) and protein (Fig. 2*C*) is present in cells lacking FADD or Caspase-8, and it was indeed suppressed by respective reconstitution of FADD or Caspase-8. This constitutive expression of ZBP1 was also observed in immortalized MEF lacking FADD and RIPK3 (Fig. 2*D*) or from adult tissues from $Casp8^{+/-}Ripk3^{-/-}$ intercrosses (Fig. 2*E*), but not in cells or tissues lacking only RIPK3. We similarly examined tissues from $Casp8^{+/+}$, or $Casp8^{-/-}Mlkl^{FLAG/FLAG}$ mice, and observed high ZBP1 expression in all examined tissues (Fig. 2*F*). We then examined the role of RIPK1 in these effects. Primary MEF lacking RIPK3

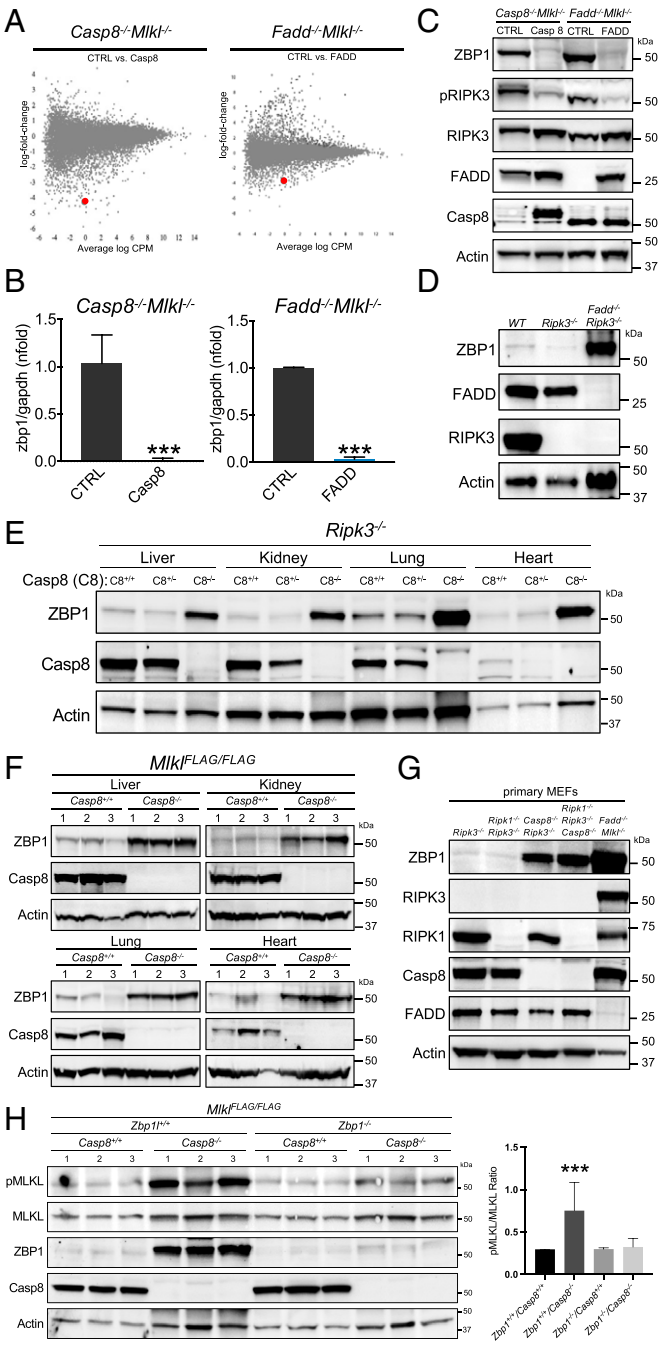

Fig. 2. *Fadd* or *Casp8* absence results in increased *Zbp1* expression. (*A*) RNA-seq analysis from $Fadd^{-/-}Mlkl^{-/-}$ or $Casp8^{-/-}Mlkl^{-/-}$ MEF reconstituted with empty vector (CTRL), FADD, or Caspase-8 (Casp8), respectively. The red bold dot is *Zbp1*. (*B*) Detection of *Zbp1* mRNA by qRT-PCR from cells as described in *A*. *Zbp1* expression was normalized using *Gapdh* mRNA levels and standardized against control (CTRL). (*C*) Cell lysates from cells described in *A*, (*D*) immortalized WT, $Ripk3^{-/-}$, or $Fadd^{-/-}Ripk3^{-/-}$ MEF, and (*E*) ZBP1 expression in liver, kidney, lung, or heart tissues from $Casp8^{+/-}Ripk3^{-/-}$ intercrosses. $Casp8^{+/+}(C8^{+/+})$; $Casp8^{+/-}(C8^{+/-})$ or $Casp8^{-/-}(C8^{-/-})$, respectively. (*F*) ZBP1 expression in kidney, liver, heart, or lung tissues from $Mlkl^{FLAG/FLAG}Casp8^{+/+}$ or $Mlkl^{FLAG/FLAG}Casp8^{-/-}$ mice was examined by immunoblotting. Numbers above panels (1 to 3) denote individual animals. (*G*) Primary $Ripk3^{-/-}$, $Ripk1^{-/-}$ $Ripk3^{-/-}$, $Casp8^{-/-}Ripk3^{-/-}$, $Ripk1^{-/-}$ $Ripk3^{-/-}Casp8^{-/-}$, and $Fadd^{-/-}Mlkl^{-/-}$ MEF were analyzed by immunoblotting using the indicated antibodies. (*H*) Immunoblotting in lung tissues from $Mlkl^{FLAG/FLAG}Zbp1^{+/+}Casp8^{+/+}$, $Mlkl^{FLAG/FLAG}Zbp1^{+/+}Casp8^{-/-}$, $Mlkl^{FLAG/FLAG}Zbp1^{-/-}Casp8^{+/+}$, and $Mlkl^{FLAG/FLAG}Zbp1^{-/-}Casp8^{-/-}$ mice (*Left*). Densitometric quantification of pMLKL/MLKL ratios from three separate animals (numbers 1 to 3) (*Right*). Significance in *B* was calculated with unpaired Student's *t* test or (*H*) two-way ANOVA analysis including a Tukey's multiple comparison test, $***P < 0.001$.

with or without RIPK1 did not show expression of ZBP1, but cells lacking Caspase-8, with or without RIPK1, expressed ZBP1 (Fig. 2*G*). Therefore, RIPK1 is not required for the expression of ZBP1 in the absence of Caspase-8 or FADD, nor is it required for suppression of such expression.

We then tested the effects of ZBP1 ablation in these settings. Using CRSPR/cas9, we ablated *Zbp1* in immortalized MEF lacking FADD and MLKL and observed that this decreased the constitutive phosphorylation of RIPK1 and RIPK3 (*SI Appendix*, Fig. S2*A*). In addition, ablation of ZBP1 in these cells prevented cell death in response to MLKL expression, although the cells remained sensitive to treatment with poly I:C plus zVAD (*SI Appendix*, Fig. S2*A*). We then crossed $Zbp1^{-/-}$ mice with $Mlkl^{FLAG/FLAG}$ mice, with or without *casp8*. Strikingly, the lack of ZBP1 reduced the phosphorylation of MLKL observed in lungs (Fig. 2*H* and *SI Appendix*, Fig. S2*B*) and livers (*SI Appendix*, Fig. S2*C*) of animals lacking both alleles of *Casp8*. Based on these findings, we suggest that the expression of ZBP1 and its activation of RIPK3 in adult tissues of $Casp8^{-/-}Mlkl^{FLAG/FLAG}$ mice is a major driver of MLKL phosphorylation in these tissues.

Nucleic Acid Sensing by ZBP1 Is Essential for RIPK3-MLKL Pathway Activity. Using our immortalized $Fadd^{-/-}Mlkl^{-/-}Zbp1^{-/-}$ MEF, we ectopically expressed *zbp1* and observed that the constitutive phosphorylation of RIPK1 and RIPK3 seen in $Fadd^{-/-}Mlkl^{-/-}$ cells was restored (Fig. 3*A*). ZBP1 contains two Zα domains (Zα1 and Zα2) (Fig. 3*B*), required for nucleic acid sensing (26), as well as an RHIM required for binding and activation of RIPK3 (6). We found that while expression of wild-type ZBP1 restored RIPK3 phosphorylation in $Fadd^{-/-}Mlkl^{-/-}Zbp1^{-/-}$ cells, deletion mutants lacking the RHIM or Zα2 did not (Fig. 3*C*). Consistent with this, we found that Dox-induced MLKL rapidly caused cell death in MEF expressing wild-type, but not the deletion mutants of ZBP1, and this cell death was prevented by inhibition of RIPK3 by GSK′872 (Fig. 3*D*). The $Fadd^{-/-}Mlkl^{-/-}Zbp1^{-/-}$ cells were nevertheless sensitive to induction of cell death (*SI Appendix*, Fig. S3*A*) and phospho-RIPK3 (*SI Appendix*, Fig. S3*B*) by treatment with TNF or poly I:C. We then expressed FLAG-ZBP1 in $Fadd^{-/-}Mlkl^{-/-}Zbp1^{-/-}$ cells reconstituted with wild-type or mutant ZBP1. We found that only in the presence of wild-type ZBP1 did phospho-RIPK3, RIPK3, and RIPK1 coprecipitate

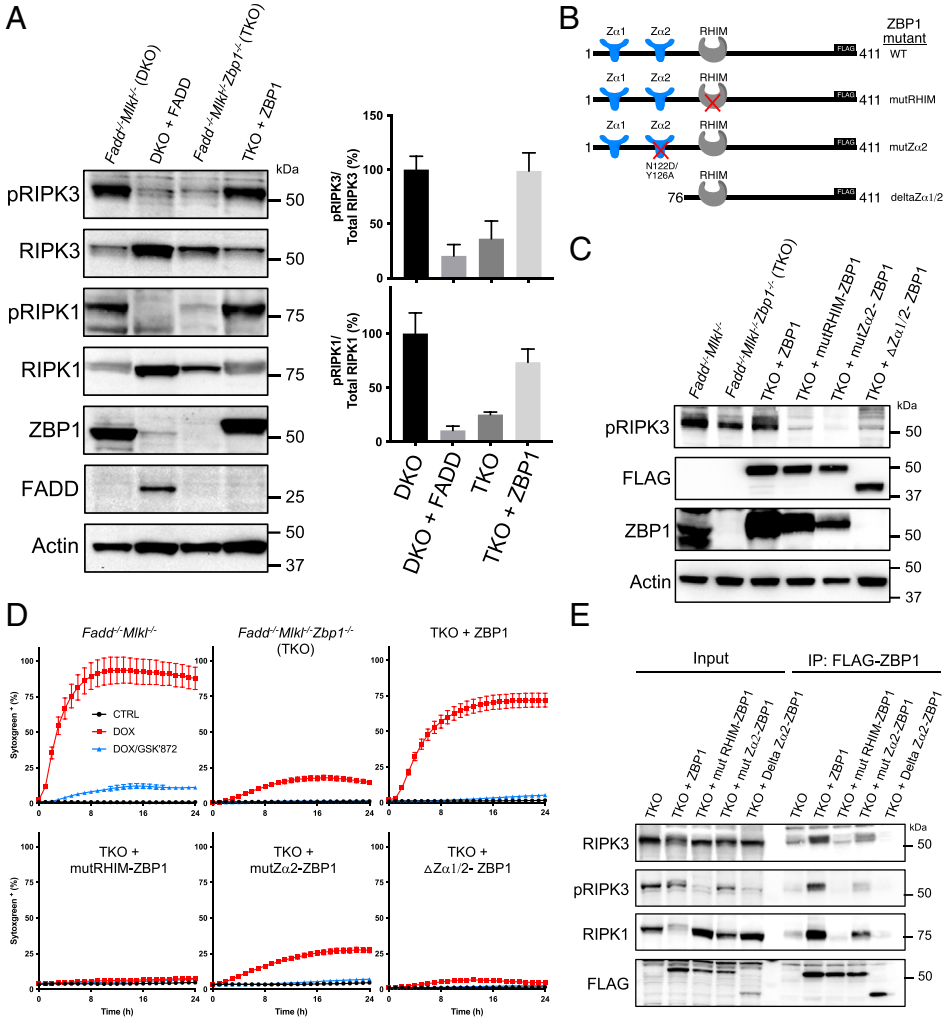

Fig. 3. ZBP1 nucleic acid sensing is required to activate RIPK3 in the absence of FADD. (*A–E*) $Fadd^{-/-}Mlkl^{-/-}$ or $Fadd^{-/-}Mlkl^{-/-}$ $Zbp1^{-/-}$ MEF were reconstituted with iMLKL-FLAG (C terminal). (*A*) $Fadd^{-/-}Mlkl^{-/-}$ MEF reconstituted with empty vector or FADD, and $Fadd^{-/-}Mlkl^{-/-}Zbp1^{-/-}$ MEF reconstituted with ZBP1. Immunoblot analysis of pRIPK1 or pRIPK3 (*Left*). Densitometric quantification of pRIPK3 (*Upper Right*) and pRIPK1 (*Lower Right*). Ratios (pRIPKs/RIPKs) were normalized to $Fadd^{-/-}Mlkl^{-/-}$ cells, which was set at 100%. (*B*) Structure of mouse ZBP1 wild-type or mutants (WT, RHIM mutant [mutRHIM], Zα2 mutant [mutZα2], and deleted Zα1/2 domains [ΔZα1/2]). (*C*) Immunoblot analysis of reconstituted ZBP1 constructs shown in *B* in $Fadd^{-/-}Mlkl^{-/-}Zbp1^{-/-}$MEF. (*D*) Cells described in *C* were incubated with Dox (1 μg/mL) or in combination with GSK′872 (1 μM). Kinetics of cell death was monitored with Sytoxgreen (Sytoxgreen^{+}, %) uptake. (*E*) Immunoprecipitation of FLAG-ZBP1 in MEF. Immunoblot of pRIPK3, RIPK3, and RIPK1 coprecipitates. Representation of two (*C* and *E*) or three independent experiments (*A* and *D*).

with ZBP1 (Fig. 3*E*). Therefore, ZBP1 appears to be responsible for activating RIPK3 in cells lacking FADD or Caspase-8.

The failure of ZBP1 lacking Zα2 to activate RIPK3 and necroptosis, despite the presence of the RHIM domain, suggests that ZBP1 must be engaged by its ligand to perform this function. As the Zα domains of ZBP1 sense Z-form nucleic acids, such as Z-RNA (26), we asked if levels of endogenous Z-RNA species are regulated by the FADD/Caspase-8 complex. We employed antibodies specific for Z-RNA or A-RNA and examined FADD- and Caspase-8–deficient cells for the presence of these double-stranded RNA species by confocal microscopy, as described previously (10, 27). We found that both *Fadd*$^{-/-}$*Mlkl*$^{-/-}$ and *Casp8*$^{-/-}$*Mlkl*$^{-/-}$ cells displayed elevated expression of Z-RNA and A-RNA that was suppressed by FADD or Caspase-8, respectively (Fig. 4). Although it has been suggested that ZBP1 recognizes mRNA from endogenous retroviruses, we did not detect such transcripts in our RNA-seq data (Gene Expression Omnibus [GEO] GSE208744). Nevertheless, based on our findings, it is likely that RNA transcripts suppressed by FADD/Caspase-8 include those capable of forming Z-RNA.

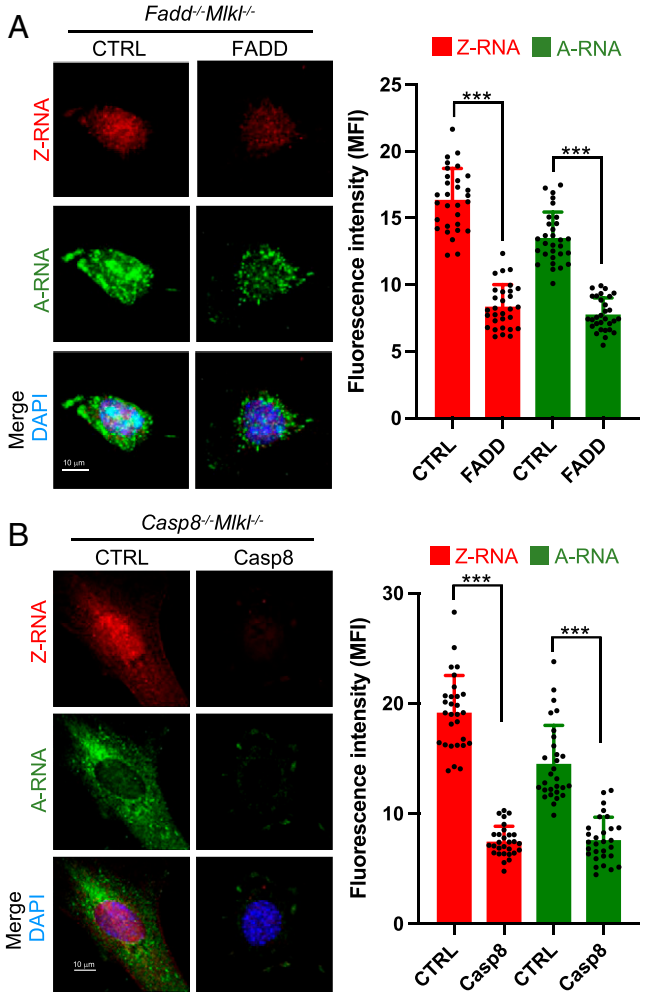

Fig. 4. Cells lacking FADD or Caspase-8 contain constitutive expression of Z-RNA. (*A*) *Fadd*$^{-/-}$*Mlkl*$^{-/-}$ or (*B*) *Casp8*$^{-/-}$*Mlkl*$^{-/-}$ MEF were reconstituted with empty vector (CTRL), FADD, or Caspase-8 (Casp8), respectively. Representative images of Z-RNA (red) or A-RNA (green) for *Fadd*$^{-/-}$*Mlkl*$^{-/-}$ (*A*) and *Casp8*$^{-/-}$*Mlkl*$^{-/-}$(*B*). Columns are quantification of MFI compiled from three independent experiments. Dots represent individual cells (*SI Appendix, SI Materials and Methods*). Significance was calculated with two-way ANOVA analysis including a Tukey's multiple comparison test, ***$P < 0.001$.

A Positive Feedback Loop Involving the cGAS-STING-TBK1 Pathway and ZBP1 in Cells Lacking Caspase-8 or FADD. *Zbp1* is an interferon response gene (28) and ZBP1 is also capable of inducing type I interferon expression via activation of TANK-binding kinase-1 (TBK1) (29). We therefore examined the phosphorylation status of TBK1 and signal transducer and activator of transcription-1 (STAT1) in our cells. *Fadd*$^{-/-}$*Mlkl*$^{-/-}$ MEF exhibited robust phospho-TBK1 and phospho-STAT1 signal, as shown by immunoblotting, which was reduced upon expression of FADD or by ablation of *zbp1* (Fig. 5*A*). Expression of ZBP1, but not ZBP1 lacking the Zα domains, restored both phospho-TBK1 and phospho-STAT1 expression in the *Fadd*$^{-/-}$*Mlkl*$^{-/-}$*Zbp1*$^{-/-}$ MEF (Fig. 5*A*). Inhibition of TBK1 kinase activity reduced ZBP1 expression (*SI Appendix*, Fig. S4*A*), suggesting the possibility of a positive feedback effect wherein ZBP1 activates TBK1, which in turn enforces ZBP1 expression.

To identify how the interferon response, leading to ZBP1 expression, might be triggered in our *Fadd*$^{-/-}$*Mlkl*$^{-/-}$ MEF, we silenced several genes using siRNA (Fig. 5*B* and *SI Appendix*, Fig. S4*B*). In agreement with our observations using a TBK inhibitor, we observed decreased ZBP1 expression upon silencing TBK1 or the type I interferon receptor IFNAR. We also found that silencing of cGAS or STING expression reduced ZBP1 levels in these cells. We observed a slight reduction in the levels of these proteins upon expression of FADD or Caspase-8, respectively, in *Fadd*$^{-/-}$*Mlkl*$^{-/-}$ or *Casp8*$^{-/-}$*Mlkl*$^{-/-}$ cells (Fig. 5*D* and *SI Appendix*, Fig. S4*C*). Accordingly, we found that the levels of cGAMP, the product of cGAS, were reduced by FADD/Caspase-8 expression (Fig. 5*E*).

We therefore ablated cGAS in *Casp8*$^{-/-}$*Mlkl*$^{-/-}$ cells (Fig. 5 *F* and *G*). We found that induced expression of MLKL resulted in rapid cell death in *casp8*$^{-/-}$*mlkl*$^{-/-}$ cells that was prevented by ablation of cGAS (Fig. 5*F*). Expression of Caspase-8 or ablation of cGAS reduced the levels of ZBP1, phospho-TBK1, and phospho-RIPK3. Reexpression of cGAS in the *Casp8*$^{-/-}$*Mlkl*$^{-/-}$*Cgas*$^{-/-}$ cells reversed these effects (Fig. 5 *F* and *G*). Similarly, ablation of STING in *Fadd*$^{-/-}$*Mlkl*$^{-/-}$ MEF reduced the levels of ZBP1, phosphorylated TBK1 and RIPK3, and prevented cell death upon reexpression of MLKL (*SI Appendix*, Fig. S5 *A* and *B*).

Interestingly, immunoprecipitation of ZBP1 in *Casp8*$^{-/-}$*Mlkl*$^{-/-}$ MEF coprecipitated TBK1, cGAS, and IRF7, as well as RIPK1, RIPK3, and FADD. This coprecipitation was not observed in wild-type MEF overexpressing a previously described (12) ZBP1 fusion protein. Restoration of Caspase-8 completely abolished coprecipitation of these proteins from the *Casp8*$^{-/-}$*Mlkl*$^{-/-}$ MEF (Fig. 5*C*).

Discussion

We found that cells lacking Caspase-8 or FADD, as well as MLKL, have constitutive activation of RIPK3 as evidenced by the presence of autophosphorylated RIPK3. Consistent with this, induced expression of ectopic MLKL rapidly triggers cell death in these cells. Mice with inactive MLKL because of insertion of an N-terminal FLAG are fully protected from embryonic lethality caused by Caspase-8 ablation, as are *Casp8*$^{-/-}$*Mlkl*$^{-/-}$ mice (16, 30). In these animals, p-MLKL was identified in all tissues examined, although this should not be interpreted as MLKL activation of all cell types within these tissues. For example, deletion of Caspase-8 in hepatocytes (31), or cardiac myocytes (15), does not cause developmental abnormalities, suggesting that MLKL is not activated in these cell types, despite our observation that liver and heart showed p-MLKL in our

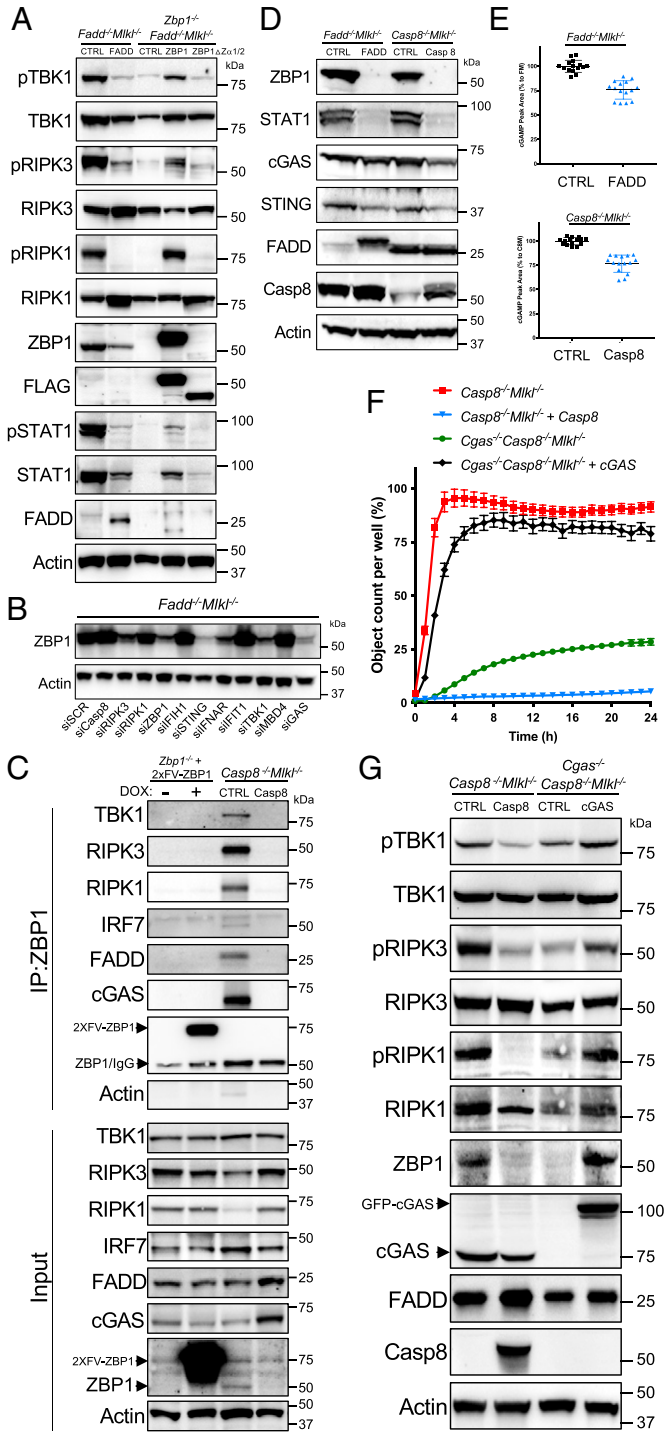

Fig. 5. The absence of FADD or Caspase-8 promotes a positive feedback loop involving the cGAS-STING and TBK1 pathways inducing ZBP1 expression. (*A*) *Fadd*$^{-/-}$*Mlkl*$^{-/-}$ MEF expressing empty vector (CTRL) or FADD, and *Fadd*$^{-/-}$*Mlkl*$^{-/-}$*Zbp1*$^{-/-}$MEF expressing WT, or ΔZα1/2-ZBP1 were harvested under untreated conditions. Cell lysates were examined by immunoblotting analysis using the indicated antibodies. (*B*) *Fadd*$^{-/-}$*Mlkl*$^{-/-}$ MEF were transiently transfected with the indicated siRNA. Forty-eight hours after transfection, cell lysates were immunoblotted for ZBP1 and actin as loading control. (*C*) Immunoprecipitation of FLAG-ZBP1 in *Zbp1*$^{-/-}$ MEF reconstituted with empty vector (CTRL) or a Dox-inducible FLAG-ZBP1 (used as internal control), and *Casp8*$^{-/-}$*Mlkl*$^{-/-}$ MEF expressing empty vector (CTRL) or Casp8. Endogenous coprecipitated proteins were assessed by immunoblotting with the indicated antibodies. (*D* and *E*) *Fadd*$^{-/-}$*Mlkl*$^{-/-}$ or *Casp8*$^{-/-}$*Mlkl*$^{-/-}$ MEF reconstituted with empty vector (CTRL), FADD, or Casp8, respectively, were harvested for liquid-chromatography/mass spectrometry quantification of cGAMP (*SI Appendix, SI Materials and Methods*). (*D*) Immunoblots of cells in (*E*, *Left*). (*E*) Dots represent cGAMP peak relative to its respective control cells (*SI Appendix, SI Materials and Methods*). Compiled from three independent experiments. (*F*) Quantification of cell death and (*G*) immunoblot analysis of endogenous components in *Casp8*$^{-/-}$*Mlkl*$^{-/-}$ or *Cgas*$^{-/-}$*Casp8*$^{-/-}$*Mlkl*$^{-/-}$ MEF versus reconstituted cells with control (CTRL), Casp8, or GFP-cGAS, respectively.

Casp8$^{-/-}$*Mlkl*$^{FLAG/FLAG}$ mice. Presumably, other cell types in these tissues were responsible for our observations.

The phosphorylation of MLKL on its activation loop is mediated by active RIPK3 (24). RIPK3 is activated by dimerization via binding of upstream RHIM-containing adaptors to its RHIM, and to date, the only proteins known to do this are RIPK1, TRIF, and ZBP1 (32). We found that in cells or tissues lacking Caspase-8 or FADD, together with the absence of functional MLKL, the constitutive activation of RIPK3 was dependent on ZBP1. Therefore, while TNF-induced RIPK1 activity and TLR-induced TRIF activation are presumably active in vivo, these appear to have at best a minor contribution to the constitutive activity of RIPK3, as evidenced by phosphorylation of the endogenous FLAG-MLKL, when Caspase-8 is globally ablated in those tissues examined (lung and liver). Recent studies support roles for ZBP1 in necroptosis induced by ablation of Caspase-8 in intestinal epithelium (33), and in skin and intestines of mice with mutations in RIPK1 (9). It remains possible, however, that RIPK3 may be active in our *Zbp1*$^{-/-}$*Casp8*$^{-/-}$*Mlkl*$^{FLAG/FLAG}$ animals in other tissues than we examined, perhaps due to the engagement of RIPK1 or TRIF, and indeed, other studies support roles for such stimuli in necroptosis induced by ablation of Caspase-8 in skin and intestine (17, 34).

Zbp1 is an interferon responsive gene (29), and we found that *Zbp1* mRNA and ZBP1 protein are expressed in cells and tissues lacking FADD or Caspase-8. This expression was suppressed upon ectopic restoration of FADD/Caspase-8 in cells. In MEF, this expression was largely dependent on cGAS and STING, the latter of which induces type I interferon (35), which presumably drove ZBP1 expression. Both cGAS and STING have been described to be targets of caspase cleavage (36, 37). We observed a slight reduction in cGAS upon reexpression of FADD-Caspase-8 in the corresponding deficient MEF, and it is possible that this represents the small proportion of cGAS responsible to produce its product, cGAMP, we observed in cells lacking FADD or Caspase-8.

Intriguingly, while cGAS-STING appeared to be required for ZBP1 expression, the ablation of ZBP1 decreased interferon signaling, as evidenced by loss of constitutive p-STAT1. Both STING and ZBP1 induce type I interferon by the activation of TBK1 (28, 38), and inhibition of TBK1 prevented both ZBP1 expression and STAT1 phosphorylation. This suggests the possibility that induction of cGAS-STING induces ZBP1, that in turn generates positive feedback via interferon production that sustains ZBP1 expression (*SI Appendix*, Fig. S4*D*). How cGAS is initiated in this pathway, however, is unclear. FADD and Caspase-8 have been described to promote DNA repair (39, 40), and cells and tissues lacking Caspase-8 accumulate DNA damage (39). It is possible that a defect in DNA repair may contribute to cGAS activation in cells lacking FADD or Caspase-8, although this is unproven.

Although ZBP1 is expressed in cells and tissues lacking FADD or Caspase-8, the function of ZBP1 to promote RIPK3 activation and MLKL phosphorylation requires the Zα domains of ZBP1, suggesting that the protein must sense its cytosolic ligand, Z-RNA, to promote RIPK3 activation (11). In line with this, we detected an elevation in both Z-RNA and

A-RNA in MEF lacking FADD or Caspase-8, which was suppressed upon reexpression of these proteins. While retroviruses are known to express mRNAs that can attain Z-RNA conformation (41), we did not detect retroviral transcripts that were regulated by Caspase-8 (GEO GSE208744). It remains possible that Z-RNA expressed in our FADD- or Caspase-8–deficient cells are due to activation of unknown, endogenous viruses, or represent transcripts of murine genes, perhaps those induced by interferon signaling.

While ZBP1 is largely considered a sensor of viral infection (8), there is evidence that it functions in other settings. For example, one study investigated MLKL-dependent necrosis in breast cancers and concluded that ZBP1 was responsible for driving the activation of MLKL (42). Our findings support the idea that the expression of ZBP1 and its activation are tightly regulated by the function of Caspase-8 under homeostatic conditions.

Materials and Methods

Generation of *Mlkl*$^{FLAG/FLAG}$ Mice. All animal use was approved by the St. Jude Children's Research Hospital institutional animal care and use committee. Insertion of FLAG tag at amino-terminal of MLKL (N-terminal FLAG-MLKL) was engineered by using CRISPR/Cas9 technology. The single-guide RNAs (sgRNAs) and Cas9 mRNA transcripts were designed and generated as described previously (43). The target site for each sgRNA is unique in the mouse genome, and no potential off-target site with fewer than two mismatches was found using the Cas-OFFinder algorithm (44). Briefly, the St. Jude Transgenic/Gene Knockout Shared Resource injected pronuclear-staged C57BL/6J zygotes with a sgRNA (5′-CTTTCAGCTATGGATAAATT-3′; 125 ng/μL) introducing a DNA double-stranded break into exon 1 of the *Mlkl* gene, human codon-optimized Cas9 mRNA transcripts (50 ng/μL), and a 154- nucleotide single-stranded DNA molecule containing the desired insertion of the FLAG tag sequence immediately after the initiator methionine (N-terminal FLAG-MLKL-HDR [homology-directed repair], 5′Cgactgaataacagatacacaggggattgtggtatttcaacca gtctatgcatctctttcagctatgGattataaagacgatgacgataaggataaattgggacagatcatcaagttaggc cagctcatctatgaacagtgtgaaaagatgaaa-3′). To facilitate the identification of founder mice and genotyping, silent substitutions generating a PsiI restriction site (5′-TTATAA-3′) were also introduced. Zygotes were surgically transplanted into the oviducts of pseudopregnant CD1 females, and newborn mice carrying the N-terminal *FLAG-Mlkl* allele were identified by PCR, PsiI-restriction digestion, and Sanger sequencing by using forward 5′-gctcctctccttgcaaacct-3′ and reverse 5′-ctggctggctgacatctgaa-3′ primers, respectively.

Tissue Immunofluorescence for pSer345-MLKL. Lung tissues were freshly collected following intratracheal inflation using 50% OCT in PBS, and immediately frozen in OCT embedding media. Tissues were cryosectioned onto charged slides and allowed to dry at room temperature for 10 min. Slides were rehydrated in PBS for 10 min at room temperature prior to blocking of endogenous biotin with an avidin/biotin kit (SP-2001; Vector Labs) followed by blocking of endogenous mouse IgG using a Mouse-on-Mouse blocking kit (Vector Labs; BMK-2202) following the manufacturer's directions. Slides were incubated overnight at 4 °C in buffer containing 4 μg/mL of monoclonal anti-pSer345-MLKL (MABC1158; Sigma). Sections were washed in PBS followed by incubation with dylight 488-labeled tomato lectin (Vector Labs; DL-1174) and Alexa Fluor 568-labeled streptavidin (S11226; ThermoFisher). Slides were washed and mounted with hard-set mounting media (P36981; Thermofisher) and imaged using a Marianas spinning disk confocal microscope (Intelligent Imaging Innovations) comprised of a CSU-W with SoRa (Yokogawa), Prime95B cMOS camera (Photometrics), 40× 1.3 NA oil objective, and Slidebook acquisition and analysis software (Intelligent Imaging Innovations).

Detection of Z-RNA/A-RNA by Immunofluorescence. Cells were plated on eight-well glass slides (EMD Millipore) and allowed to adhere for at least 24 h before use in experiments. As previously described (45), cells were fixed for 10 min with freshly prepared 4% (wt/vol) paraformaldehyde in PBS, permeabilized in 0.5% (vol/vol) Triton X-100 in PBS, blocked with MAXblock Blocking Medium (Active Motif), and incubated overnight with primary antibodies at 4 °C. After three washes in PBS, slides were incubated with fluorophore-conjugated secondary antibodies for 1 h at room temperature. Following an additional three washes in PBS, slides were mounted in ProLong Gold antifade reagent (Thermo Fisher Scientific) and imaged by confocal microscopy on a Leica SP8 instrument. Thirty cells from duplicated wells were selected randomly and detected the fluorescence intensity of Z-RNA (red channel) and A-RNA (green channel). Mean fluorescence intensity was quantified using Leica LAS X software. Primary antibodies were used for immunofluorescence studies: Z-RNA (clone Z22, Absolute Antibody; dilution: 1:200), A-RNA (clone 9D5; Millipore; dilution: 1:50).

Data, Materials, and Software Availability. RNA-seq data have been deposited in the National Center for Biotechnology GEO database, https://www.ncbi.nlm.nih.gov/geo (accession no GSE208744) (46). All other study data are included in the main text and *SI Appendix*.

ACKNOWLEDGMENTS. We thank Dr. Joelle Magne, Dr. Mao Yang, Dr. Katherine Verbist, and Shyam Sirasanagandla for invaluable support and discussions. This work was supported by the American Lebanese Syrian Associated Charities (St. Jude Children's Research Hospital), and by US National Cancer Institute Grant R35 CA231620 and NIH Grant AI44828 (to D.R.G.), and NIH Cancer Center Support Grant P30 CA021765. Work in the S.B. laboratory was supported by NIH Grants AI135025 and AI144400, and by NIH Cancer Center Support Grant P30CA006927. This work was also supported by the German Research Foundation (DFG, KA 4830/1-1) (to H.K.).

Author affiliations: [a]Department of Immunology, St. Jude Children's Research Hospital, Memphis, TN, 38105; and [b]Blood Cell Development and Function Program, Fox Chase Cancer Center, Philadelphia, PA, 19111

1. J. Zhao *et al.*, Mixed lineage kinase domain-like is a key receptor interacting protein 3 downstream component of TNF-induced necrosis. *Proc. Natl. Acad. Sci. U.S.A.* **109**, 5322–5327 (2012).
2. L. Sun *et al.*, Mixed lineage kinase domain-like protein mediates necrosis signaling downstream of RIP3 kinase. *Cell* **148**, 213–227 (2012).
3. M. A. Kelliher *et al.*, The death domain kinase RIP mediates the TNF-induced NF-kappaB signal. *Immunity* **8**, 297–303 (1998).
4. S. Orozco *et al.*, RIPK1 both positively and negatively regulates RIPK3 oligomerization and necroptosis. *Cell Death Differ.* **21**, 1511–1521 (2014).
5. W. J. Kaiser *et al.*, Toll-like receptor 3-mediated necrosis via TRIF, RIP3, and MLKL. *J. Biol. Chem.* **288**, 31268–31279 (2013).
6. J. W. Upton, W. J. Kaiser, E. S. Mocarski, DAI/ZBP1/DLM-1 complexes with RIP3 to mediate virus-induced programmed necrosis that is targeted by murine cytomegalovirus vIRA. *Cell Host Microbe* **11**, 290–297 (2012).
7. W. J. Kaiser, J. W. Upton, E. S. Mocarski, Receptor-interacting protein homotypic interaction motif-dependent control of NF-kappa B activation via the DNA-dependent activator of IFN regulatory factors. *J. Immunol.* **181**, 6427–6434 (2008).
8. S. Balachandran, E. S. Mocarski, Viral Z-RNA triggers ZBP1-dependent cell death. *Curr. Opin. Virol.* **51**, 134–140 (2021).
9. H. Jiao *et al.*, Z-nucleic-acid sensing triggers ZBP1-dependent necroptosis and inflammation. *Nature* **580**, 391–395 (2020).
10. T. Zhang *et al.*, Influenza virus Z-RNAs induce ZBP1-mediated necroptosis. *Cell* **180**, 1115–1129.e13 (2020).
11. T. Kuriakose *et al.*, ZBP1/DAI is an innate sensor of influenza virus triggering the NLRP3 inflammasome and programmed cell death pathways. *Sci. Immunol.* **1**, aag2045 (2016).
12. R. J. Thapa *et al.*, DAI senses influenza A virus genomic RNA and activates RIPK3-dependent cell death. *Cell Host Microbe* **20**, 674–681 (2016).
13. H. Koehler *et al.*, Inhibition of DAI-dependent necroptosis by the Z-DNA binding domain of the vaccinia virus innate immune evasion protein, E3. *Proc. Natl. Acad. Sci. U.S.A.* **114**, 11506–11511 (2017).
14. L. Wang, F. Du, X. Wang, TNF-alpha induces two distinct caspase-8 activation pathways. *Cell* **133**, 693–703 (2008).
15. A. Oberst *et al.*, Catalytic activity of the caspase-8-FLIP(L) complex inhibits RIPK3-dependent necrosis. *Nature* **471**, 363–367 (2011).
16. S. Alvarez-Diaz *et al.*, The pseudokinase MLKL and the kinase RIPK3 have distinct roles in autoimmune disease caused by loss of death-receptor-induced apoptosis. *Immunity* **45**, 513–526 (2016).
17. R. Weinlich *et al.*, Protective roles for caspase-8 and cFLIP in adult homeostasis. *Cell Rep.* **5**, 340–348 (2013).
18. N. Lalaoui *et al.*, Mutations that prevent caspase cleavage of RIPK1 cause autoinflammatory disease. *Nature* **577**, 103–108 (2020).
19. P. Tao *et al.*, A dominant autoinflammatory disease caused by non-cleavable variants of RIPK1. *Nature* **577**, 109–114 (2020).
20. K. Newton *et al.*, Cleavage of RIPK1 by caspase-8 is crucial for limiting apoptosis and necroptosis. *Nature* **574**, 428–431 (2019).

21. J. P. Ingram *et al.*, ZBP1/DAI drives RIPK3-mediated cell death induced by IFNs in the absence of RIPK1. *J. Immunol.* **203**, 1348–1355 (2019).
22. C. P. Dillon *et al.*, Survival function of the FADD-CASPASE-8-cFLIP(L) complex. *Cell Rep.* **1**, 401–407 (2012).
23. C. P. Dillon *et al.*, RIPK1 blocks early postnatal lethality mediated by caspase-8 and RIPK3. *Cell* **157**, 1189–1202 (2014).
24. D. A. Rodriguez *et al.*, Characterization of RIPK3-mediated phosphorylation of the activation loop of MLKL during necroptosis. *Cell Death Differ.* **23**, 76–88 (2016).
25. M. Rebsamen *et al.*, DAI/ZBP1 recruits RIP1 and RIP3 through RIP homotypic interaction motifs to activate NF-kappaB. *EMBO Rep.* **10**, 916–922 (2009).
26. A. Athanasiadis, Zalpha-domains: At the intersection between RNA editing and innate immunity. *Semin. Cell Dev. Biol.* **23**, 275–280 (2012).
27. C. C. Hardin, D. A. Zarling, S. K. Wolk, W. S. Ross, I. Tinoco Jr., Characterization of anti-Z-RNA polyclonal antibodies: Epitope properties and recognition of Z-DNA. *Biochemistry* **27**, 4169–4177 (1988).
28. A. Takaoka *et al.*, DAI (DLM-1/ZBP1) is a cytosolic DNA sensor and an activator of innate immune response. *Nature* **448**, 501–505 (2007).
29. K. J. Ishii *et al.*, TANK-binding kinase-1 delineates innate and adaptive immune responses to DNA vaccines. *Nature* **451**, 725–729 (2008).
30. B. Tummers *et al.*, Caspase-8-dependent inflammatory responses are controlled by its adaptor, FADD, and necroptosis. *Immunity* **52**, 994–1006.e8 (2020).
31. M. Hatting *et al.*, Hepatocyte caspase-8 is an essential modulator of steatohepatitis in rodents. *Hepatology* **57**, 2189–2201 (2013).
32. D. R. Green, The coming decade of cell death research: Five riddles. *Cell* **177**, 1094–1107 (2019).
33. R. Schwarzer, H. Jiao, L. Wachsmuth, A. Tresch, M. Pasparakis, FADD and caspase-8 regulate gut homeostasis and inflammation by controlling MLKL- and GSDMD-mediated death of intestinal epithelial cells. *Immunity* **52**, 978–993.e6 (2020).
34. D. Panayotova-Dimitrova *et al.*, cFLIP regulates skin homeostasis and protects against TNF-induced keratinocyte apoptosis. *Cell Rep.* **5**, 397–408 (2013).
35. A. Ablasser *et al.*, cGAS produces a 2′-5′-linked cyclic dinucleotide second messenger that activates STING. *Nature* **498**, 380–384 (2013).
36. Y. Xiong, Y. D. Tang, C. Zheng, The crosstalk between the caspase family and the cGAS–STING signaling pathway. *J. Mol. Cell Biol.* **13**, 739–747 (2021).
37. X. Ning *et al.*, Apoptotic caspases suppress type I interferon production via the cleavage of cGAS, MAVS, and IRF3. *Mol. Cell* **74**, 19–31.e7 (2019).
38. Y. Tanaka, Z. J. Chen, STING specifies IRF3 phosphorylation by TBK1 in the cytosolic DNA signaling pathway. *Sci. Signal.* **5**, ra20 (2012).
39. Y. Boege *et al.*, A dual role of caspase-8 in triggering and sensing proliferation-associated DNA damage, a key determinant of liver cancer development. *Cancer Cell* **32**, 342–359.e10 (2017).
40. R. A. Screaton *et al.*, Fas-associated death domain protein interacts with methyl-CpG binding domain protein 4: A potential link between genome surveillance and apoptosis. *Proc. Natl. Acad. Sci. U.S.A.* **100**, 5211–5216 (2003).
41. J. Maelfait *et al.*, Sensing of viral and endogenous RNA by ZBP1/DAI induces necroptosis. *EMBO J.* **36**, 2529–2543 (2017).
42. J. Y. Baik *et al.*, ZBP1 not RIPK1 mediates tumor necroptosis in breast cancer. *Nat. Commun.* **12**, 2666 (2021).
43. S. Pelletier, S. Gingras, D. R. Green, Mouse genome engineering via CRISPR-Cas9 for study of immune function. *Immunity* **42**, 18–27 (2015).
44. S. Bae, J. Park, J. S. Kim, Cas-OFFinder: A fast and versatile algorithm that searches for potential off-target sites of Cas9 RNA-guided endonucleases. *Bioinformatics* **30**, 1473–1475 (2014).
45. T. Zhang *et al.*, ADAR1 masks the cancer immunotherapeutic promise of ZBP1-driven necroptosis. *Nature* **606**, 594–602 (2022).
46. D. A. Rodriguez, B. Tummer, M. J. Chen, J. C. Crawford, D. R. Green, Caspase-8 and FADD prevent spontaneous ZBP1 expression and necroptosis. Gene Expression Omnibus. https://www.ncbi.nlm.nih.gov/geo/query/acc.cgi?acc=GSE208744. Deposited 19 September 2022.